Adhesion of thermally sprayed hydroxyapatite–bond-coat systems measured by a novel peel test

H. KURZWEG, R. B. HEIMANN*
Department of Mineralogy, Freiberg University of Mining and Technology, D-09599 Freiberg, Federal Republic of Germany

T. TROCZYNSKI
Department of Metals and Materials Engineering, University of British Columbia, Vancouver, BC, Canada V6T 1Z4

Ti6Al4V foils, 100 μm thick, were coated with thin (10–15 μm) bond coats based on titania and zirconia, and subsequently coated with a thick (100–120 μm) hydroxyapatite layer, using atmospheric plasma spraying. Peel adhesion tests of the coating systems performed on the foils showed that titania, and mixed titania/non-stabilized zirconia bond coats improved the adhesion of the ceramic layers to the metallic substrate in a statistically significant way, while a partially CaO-stabilized zirconia bond coat led to a decrease of the peel adhesion strength when compared to hydroxyapatite coatings without a bond coat.

1. Introduction

Bioactive ceramics, such as calcium phosphate in general, and hydroxyapatite ($C_{10}P_3H$**, HAp) in particular, are in widespread use as implant-substitute components or as interfacing layers in metallic surgical implants. Because incomplete fixation to living bone of uncoated cementless joints for total hip replacement (THP) is a common problem, application of hydroxyapatite coatings by plasma-spray processing to the surfaces of titanium alloy hip endoprosthetic implants constitutes the state-of-the-art procedure to induce osseointegration by bonding osteogenesis [1–3]. Owing to the chemical similarity of HAp to the inorganic component of the composite material "bone", its presence at the implant surface helps to develop a tight bond between implant material and living bone and is thus able to improve fixation and stability of the implant, and thus decrease recovery time after implantation.

The high temperature in a plasma jet leads inevitably to changes of the degree of crystallinity, i.e. development of amorphous calcium phosphate (ACP) and the phase composition, i.e. partial dehydration of HAp into oxyhydroxyapatite (OHAp) or oxyapatite (OAp) and thermal transformation of HAp into tri- (TCP)- or tetracalcium (tetrCP) phosphate or even non-biocompatible CaO [4]. Because these phases have a lower resorption resistance than stoichiometric HAp and also seem to decrease the adhesion strength to the metallic substrate, their occurrence must be suppressed.

The *in vivo* performance of such coatings depends on a large array of factors, most notably coating thickness, chemical composition, crystallinity, phase purity, cohesive and adhesive strengths, and resorption resistance [5]. In particular, adhesion strength of the coating to the implant surface appears to be a property that needs to be maximized to avoid cracking, shearing off, and chipping of the HAp coating during emplacement of the implant. Also, improved adhesion and resorption resistance of the coating material will prevent the formation of a gap between metal implant and coating that may promote unwanted invasion of acellular connective tissue which may, in turn, lead to aseptic loosening of the implant as a result of micromotions during the initial phase of the healing process [6]. Some limited improvement of the adhesion strength can be achieved by carefully controlling the plasma-spray parameters [7], or by microstructural engineering of the spray powder through pre-spray annealing [8]. A completely different way to achieve improved adhesion is to consider biocompatible bond coats. This paper deals with the development of biocompatible bond coats and testing of the adhesion strength of the resulting coating systems.

* Author to whom all correspondence should be addressed.
** Cement chemistry notation: C = CaO, P = P_2O_5, H = H_2O, S = SiO_2, T = TiO_2 and Z = ZrO_2.

0957–4530

2. Bond coats for bioceramic coating systems

The utilization of bond coats to increase the adhesion of wear- and corrosion-resistant coatings, as well as thermal barrier coatings, to a given substrate is well documented in the thermal-spraying literature [9]. In applications for bioceramic coatings, bond coats should also, in addition to improving adhesion strength:

(i) prevent direct contact between titanium and HAp because this is thought to catalyse the thermal transformation of HAp towards tri- or tetracalcium phosphate or even non-biotolerant CaO [10, 11];

(ii) reduce the release of metal ions from the substrate to the surrounding living tissue that has been shown to induce massive hepatic degeneration in mice [12] and impaired development of human osteoblasts [13];

(iii) reduce the thermal gradient at the substrate/coating interface caused by the rapid quenching of the molten particle splats that leads to deposition of amorphous HAp with a concurrent decrease in resorption resistance [8] and hence to reduced *in vivo* performance, i.e. longevity of the implant;

(iv) prevent a steep gradient in the coefficients of thermal expansion between substrate and coating that promotes the formation of strong tensile forces in the coating, giving rise to crack generation, chipping and/or delamination, as well as

(v) cushion damage by cracking and delamination of the coating initiated by cyclic micromotions of the implant during movement of the patient in the initial phase of the healing process [14].

Thus it is highly desirable to engineer the substrate/HAp coating interface in such a way that by application of a suitable thin biocompatible bond-coat layer the advantages addressed above can be realized.

Preliminary work indicated that the application to a Ti6Al 4V substrate of a dicalcium silicate (C_2S) bond coat (10–50 μm thick)/hydroxyapatite top coat (30–130 μm thick) system by atmospheric plasma spraying (Plasmadyne 3610-D; plasma current 700–900 A; plasma gas argon/10% helium) led to a rather small but statistically significant increase of the average adhesion strength on the order of 20% (13.7 MPa) compared to a HAp coating sprayed without a bond coat (11.4 MPa) [15]. Careful plasma-parameter optimization and use of low-pressure plasma-spray condition increased the adhesion strength in the presence of a dicalcium silicate bond coat to over 30 MPa [16]. This value, however, decreased to 20 MPa on immersion in simulated body fluid (Hank's Balanced Salt Solution, HBSS) for 7 d at 37 °C. This substantial decrease is presumably due to a hydrolysis reaction of the dicalcium silicate. Besides, hydrated soluble silica species were found to enhance proliferation of human osteoblasts and also active cellular production of transforming growth factors [17, 18]. Moreover, absorption of silica polyanions on primary, plasma-sprayed HAp surfaces may provide a biomimetic route towards crystallization of secondary HAp because these ions appear to mediate nucleation of apatite [19]. Indeed, bioactive C–S glasses producing those soluble silica species were found to bond strongly to living bone, forming an apatite surface layer when exposed to body fluid [20]. In addition, C–S bond coats have, for ceramics, exceptionally high coefficients of linear thermal expansion (CTE) ranging from $10–13 \times 10^{-6} K^{-1}$ [21]. Because the CTE of titanium is $8.5 \times 10^{-6} K^{-1}$ there is a good match and most of the residual stresses in the ceramic coating will be prevented. There is even the possibility of introducing a compressive stress component at the interface substrate/C–S bond coat supporting good adhesion [5].

Other suitable bond coats are being developed within the binary system ZrO_2–TiO_2 [22]. The plasma-spray conditions, the morphological appearance and the adhesion strength of those coating systems will be described below.

3. Peel adhesion test

The quality and in-service performance of a thermally sprayed coating is, to a large extent, determined by the quality of its adhesion to the substrate. Over the years, a large variety of different tests has been devised to measure the adhesion strength in an accurate and reproducible way. Despite of their shortcomings, related to the frequently observed infiltration of the coating by the adhesive used and the fact that in many cases separation occurs in an uncontrolled manner by the random location and movement of the crack tip within the coating, conventional tensile pull tests (ASTM C633-79, DIN 50160/10.90 or EN 582 : 1993) are still most widely used, even though there is a rather urgent call to interprete tensile adhesion tests in terms of a more appropriate design philosophy [23].

Hence it is not surprising that the adhesion strength results reported in the literature for HAp coatings produced at comparable deposition conditions, span a wide range, from below 10 to about 70 MPa [5]. The deviations have been variously explained as being due to differing test procedures [2] as well as by utilization of different adhesives [24]. Because the uncontrolled mode of coating/substrate separation in the conventional pull tests contributes, to a large extent, to the uncertainty of the test results, a modified ASTM D3167-76 peel test was introduced recently [25]. A coating is deposited on to a thin metal foil attached to a massive copper block that provides mechanical support and acts as a heat sink. The block, foil and coating assembly is glued to a stiff aluminium plate, and the copper block is then removed. Peeling off the foil from the coating, as shown in Fig. 1, causes a crack to propagate precisely along the coating/foil interface in a stable and controllable manner, because the sample geometry forces the crack tip to move along the interface [26] where it encounters the local least energy path. While the conventional tensile pull test measures failure stress, expressed as the ratio of applied force to coating area ($N m^{-2}$), the novel peel test measures the energy required to separate the coating and the foil along a line ($N m^{-1}$). Because some of the energy spent is used to deform the foil plastically during bending, this contribution must be considered

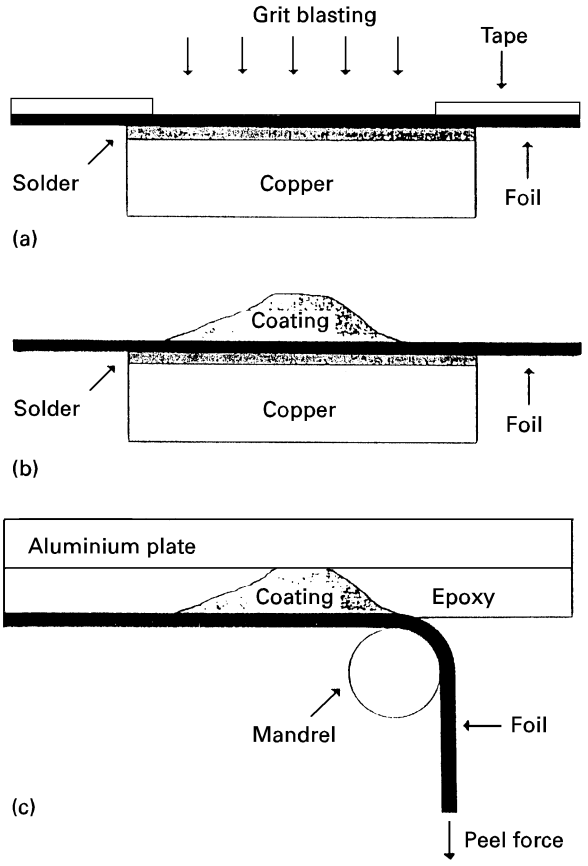

Figure 1 Schematic cross-sections of the test assembly in various stages: (a) during grit blasting, (b) after plasma spraying ready for gluing to the aluminium plate, (c) before peel testing (after [25]).

to interpret the test results properly. The work of deformation of the foil can be determined from the measured stress–strain curve of the metal [27]. Refer to the Appendix for further details on the calculation of the peel force.

4. Experimental procedure

4.1. Plasma spraying of hydroxyapatite/bond coat systems

Various hydroxyapatite/bond coat systems were plasma sprayed on to grit-blasted Ti6Al4V coupons of dimension $50 \times 20 \times 2\ mm^3$ and on to foils of dimensions $120 \times 16 \times 0.1\ mm^3$ using atmospheric plasma-spray equipment (Plasmatechnik AG, F4 torch). Grit blasting of the coupons was performed using silicon carbide (grain size range 0.71–1.0 mm) at an air pressure of 500 kPa and a distance of 50 mm from the target. Grit blasting of the foils was done using alumina grit (600–800 μm) at an air pressure of 250 kPa and a distance of 50 mm. After grit blasting, the coupons and foils were cleaned ultrasonically with acetic acid ethylester and ethyl alcohol, and attached to copper blocks using a 1:2 mixture (by weight) of a silicone sealant (Dow Corning 732) and copper powder (ALCAN 154, grain size range <44 μm). The adhesive was cured at room temperature for 12 h. The presence of copper powder in the adhesive provides, during plasma spraying, excellent conduction of heat away from the foil into the copper block acting as an effective heat sink. The type of adhesive used allows for an easy removal of the foil from the copper block for post-spray sample preparation.

Bond coats of thickness 10–15 μm, deposited on to Ti6Al4V substrate coupons and foils, consisted of partially CaO-stabilized zirconia (DYNAZIRKON C, Hüls AG, grain size 0.45–60 μm, series 2), a mechanically mixed powder of 73 mol % titania and 27 mol % non-stabilized zirconia, corresponding to the eutectic composition (Type 9303, Carl Roth GmbH, grain sizes 0.18–26 μm, series 3), and titania (AMDRY 6500, Sulzer Metco GmbH, grain size 5–22 μm, series 4). The plasma-spray parameters used are shown in Table I. Subsequently, a thick (100–120 μm) layer of hydroxyapatite (AMDRY™ 6021, Sulzer Metco Deutschland GmbH) was sprayed on to the bond coat using the parameters shown in Table II. In addition, foils were sprayed with HAp using the same parameters but without using a bond coat (series 1) to establish a bench mark for estimating the effect of the various bond coats on the adhesion behaviour.

The chemical compositions of the materials used are shown in Table III.

TABLE I Plasma-spray parameters for bond coats

Parameter	$(CaO)ZrO_2$	$TiO_2 + ZrO_2$	TiO_2
Plasma power (kW)	42.2	42.2	41.6
Plasma current (A)	630	630	630
Argon ($l\,min^{-1}$)	40	40	40
Hydrogen ($l\,min^{-1}$)	12	12	12
Carrier gas Ar ($l\,min^{-1}$)	2.6	2.6	2.6
Torch speed ($m\,min^{-1}$)	30	30	30
Stand-off distance (mm)	100	100	80
Powder feed ($g\,min^{-1}$)	18.5	23	20

TABLE II Plasma-spray parameters for HAp top coats

Parameter	HAp coat
Plasma power (kW)	25.8
Plasma current (A)	470
Argon ($l\,min^{-1}$)	50
Hydrogen ($l\,min^{-1}$)	4
Carrier gas Ar ($l\,min^{-1}$)	6
Torch speed ($m\,min^{-1}$)	30
Stand-off distance (mm)	100
Powder feed ($g\,min^{-1}$)	23.5

TABLE III Chemical composition of spray powders (mass %)

	Hydroxy-apatite	CaO-stabilized ZrO_2	TiO_2	ZrO_2
CaO	55.8	4.4		
P_2O_5	42.7			
TiO_2			98.4	
ZrO_2				99.0
$ZrO_2 + HfO_2$		94.9		
Other oxides	1.5	0.7	1.6	1.0

4.2. Peel adhesion test

After plasma spraying the Ti6Al4V foils, the sample assembly shown schematically in Fig. 1 was fixed to a stiff aluminium plate of dimensions $120 \times 16 \times 2\,mm^3$ with epoxy resin (HYSOL EA 934 NA, Hysol Aerospace Products), and the copper block was removed. The coated titanium foil/epoxy/aluminium plate assembly was mounted on a jig (for a detailed description, see [25]) in an Instron 4200 universal testing machine (Instron Corporation, Canton, MA). The end of the foil was clamped to the upper grip of the machine and pulled away from the coating at a constant rate of $2.5\,mm\,min^{-1}$. The load and the crosshead displacement were recorded digitally, and corresponding stress–strain curve calculated from the recorded data. Different deadweights were attached to the other end of the foil in order to make the foil conform to the mandrel of the jig (Fig. 2). The peeling force was averaged over 5–10 mm crosshead displacement, and more weight was added as the test progressed. Because the measured force is the sum of the peel force, the deadweight, the frictional force and the plastic work per increment peeled [27], from a plot of the measured force versus the known deadweight, the peel force can be obtained as shown in detail in the Appendix.

4.3. Microstructural investigations

The microstructure and chemical composition of the hydroxyapatite/bond-coat systems plasma sprayed to Ti6Al4V coupons were investigated using a scanning electron microscope (Hitachi S2700) in conjunction with an energy-dispersive X-ray detection system (Link eXL). Scanning electron microscopy was also employed to investigate separated titanium alloy foil–aluminium plate/epoxy/coating assemblies to ascertain at which of the two interfaces (titanium alloy substrate/bond coat or bond coat/HAp top coat) separation had occurred.

Samples were prepared by cutting a 5 mm slice from the coated coupon ($50 \times 20 \times 2\,mm^3$) using a low-speed diamond wheel. This slice was cut in half and the two pieces were glued together coating-to-coating with epoxy resin loaded with nickel powder (20–100 μm) to maintain good edge retention during the subsequent grinding and polishing cycles. Some samples were also prepared with a thin nickel strip embedded in the epoxy and separating the coatings. The sample sandwich was then embedded in thermoplastic acrylic resin (Lucite) and the surface ground with silicon carbide paper (600 and 1200) using the "trailing edge technique" in which the specimen is abraded only in the direction perpendicular to the edge of interest. Weak pressure (7–13 N for a 1 in. (2.54 cm) diameter sample) was applied only during the stroke in which this edge is the trailing edge. The sample was lifted off the surface of the silicon carbide paper at the end of the stroke and was returned to the start of the stroke without contacting the paper surface [31]. This tedious procedure yielded, in conjunction with the nickel-loaded epoxy or the nickel strip, excellent edge retention during grinding of materials with very dissimilar hardnesses and abrasion rates, such as the layered succession of titanium, ceramic bond coat, HAp top coat, and epoxy resin. Polishing was done on nylon cloth using 6 μm diamond paste, followed by a slurry of magnesium oxide on short-napped cloth.

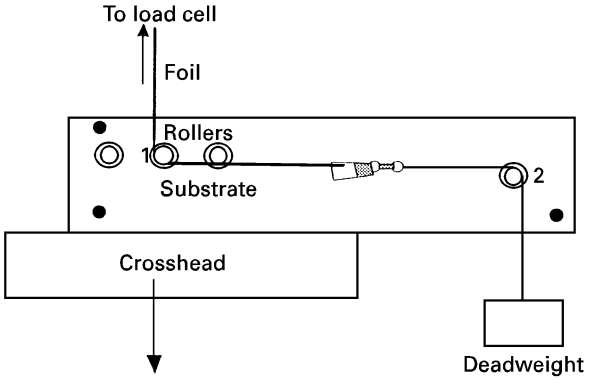

Figure 2 Peel adhesion test loading jig with deadweight applied to make the foil conform to the curvature of the rollers (after [27]).

5. Results and discussion

Fig. 3 shows typical results of the peel adhesion test. Here the normalized total force (F/w) is plotted against deadweight (D/w) from which lines the normalized peel strengths (G/w) of a hydroxyapatite coating without a bond coat (series 1, Fig. 3a) and a hydroxyapatite/titania bond coat system (series 4, Fig. 3b) were calculated. The calculated peel strengths of all samples are shown in Table IV together with the relevant linear regression lines $y = a + bx$, where x is the normalized deadweight D/w.

Based on the comparison of the intersection with the y-axes, (a) of series 1 (no bond coat) to series i ($i = 2, 3, 4$), a significance test was done [32]. The calculated $|t_r^{(a)}|$-values are always higher than the tabulated $t_{m,q}$ values for m degrees of freedom and a level of confidence $\alpha = 0.05$. These values are also included in Table IV. Thus there is a significant difference between the peel strengths. It can be shown that series 2 (CaO-stabilized zirconia) has a significantly lower peel adhesion strength than the HAp coating without a bond coat. On the other hand, the results for series 3 (titania/zirconia bond coat) and 4 (titania) show that those bond coats improve the peel adhesion strength in a statistically significant way. In particular, a titania bond coat leads to a peel strength twice the value of an HAp coat without a bond coat. The reason for this behaviour may be seen in the development of a thin reaction zone at the immediate interface between bond coat and HAp top coat consisting of calcium titanates and/or zirconates [33]. Calcium titanates have been reported to occur at the interface of a titanium substrate terminated by a thin layer of native oxide and a HAp coating by de Groot *et al.* [1] (perovskite, CT) and Ji *et al.* [11] (calcium dititanate, CT_2). Perovskite and calcium zirconate (CZ) ceramics implanted intramusculatory in rabbits showed the development of a 100–200 μm thick pseudomembrane that with time (6–9 mon) densified gradually. The

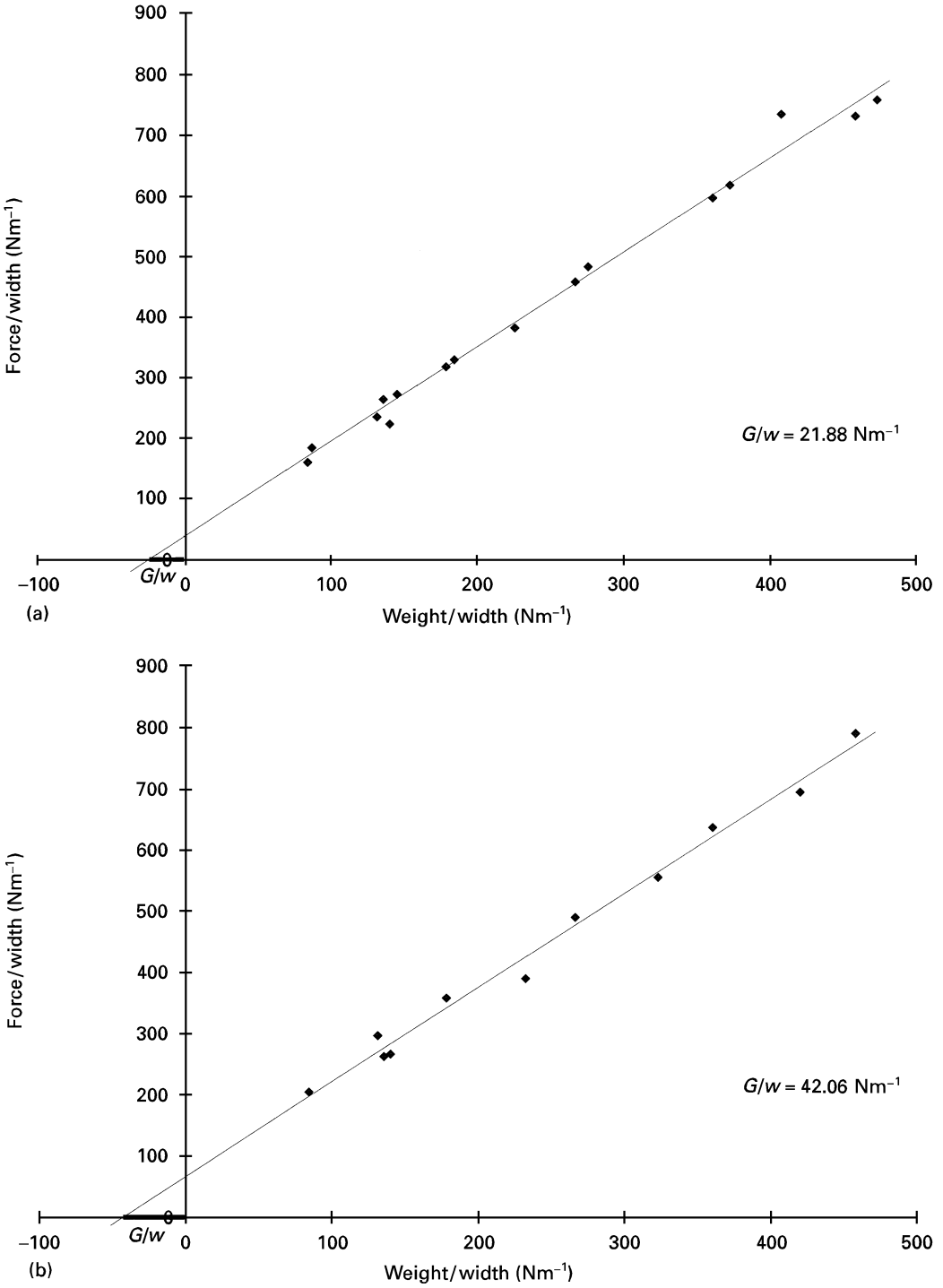

Figure 3 Plots of the normalized total force (F/w) versus the normalized deadweight (D/w) to determine the peel strength (G/w) of coatings. (a) HAp coating without a bond coat, (b) HAp top coat/titania bond coat system.

absence of inflammatory cells suggested a high degree of biotolerance of these ceramic materials [34]. Also, calcium atoms in HAp may be partially replaced by titanium ions forming titanium-substituted hydroxyapatite, $Ca_{10-n}Ti_{n/2}[(PO_4)_6(OH)_2]$ or, at higher titanium concentrations, titanium hydrogenphosphate of the type $Ti(HPO_4)_2$ [35], hence providing a kind of chemical bond that will strengthen adhesion over and above that obtained by simple mechanical interlocking of the molten particle splats into asperities of the grit-blasted substrate surface. EDX analyses done close to the interface bond coat/HAp top coat did not reveal any distinct reaction zones. Because it is expected that any reaction layer will be extremely thin, other analytical techniques must be employed, such as transmission electron microscopy (TEM), and/or surface analytical techniques, such as Auger, SIMS or photo-electron spectroscopy. Such investigations are in progress.

Fig. 4 shows scanning electron micrographs of polished cross-sections of as-sprayed hydroxyapatite/bond-coat systems. Fig. 4a shows the titanium alloy substrate (right), a thin CaO-stabilized zirconia bond coat (centre) and the HAp top coat (left) (series 2). The bond coat exhibits microcracks, perpendicular to the interface, and also longitudinal cracks,

TABLE IV Calculated peel strengths for the coating systems investigated

Series	Regression line	Peel strength ($N\,m^{-1}$)	$\lvert t_r^{(a)} \rvert$	$t_{m,q}$
1	$y = 34.7 + 1.59x$	21.9	–	–
2	$y = 30.3 + 1.68x$	18.0	2.54	2.07
3	$y = 51.1 + 1.61x$	31.8	2.15	2.06
4	$y = 65.2 + 1.55x$	42.1	2.67	2.07

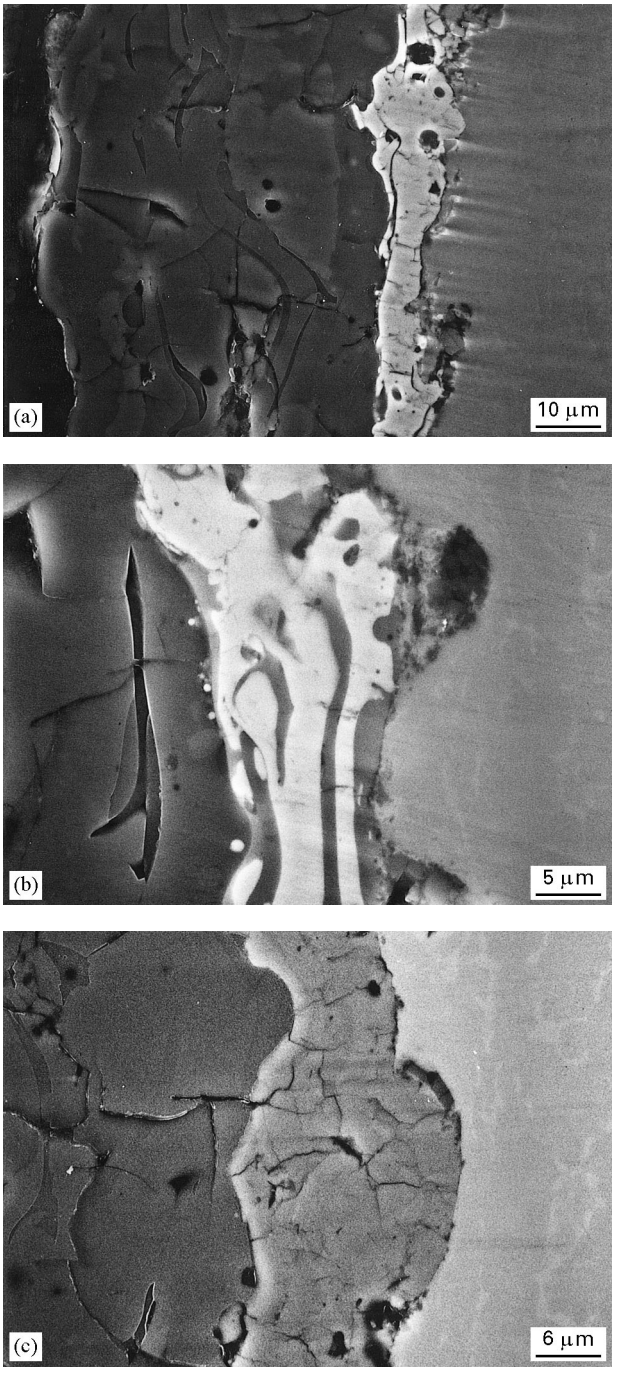

Figure 4 Polished scanning electron micrographs of plasma-sprayed hydroxyapatite/bond-coat systems. (a) Calcium-stabilized zirconia bond coat, (b) bond coat of a mechanical mixture of 73 mol % titania and 27 mol % zirconia (eutectic composition), (c) titania bond coat.

parallel to the interface, that may originate from the mismatch in the coefficients of thermal expansion of the metal and the ceramics. It is these cracks that limit the adhesion of the coating system during the peel test and lead to pronounced coating delamination. As shown above, coating systems of series 2 have peel strengths significantly lower than that of HAp coatings without a bond coat. This is somewhat in discord with results obtained by Matejka [36] who used stabilized zirconia bond coats to improve the biomechanical performance of dental implants of various shapes. They found that such zirconia-HAp systems survived well in dogs and humans for periods of up to 5 y.

Fig. 4b shows a cross-sectional view of a coating system (series 3) consisting of the titanium alloy substrate (right), a mixed zirconia/titania bond coat (centre) and the HAp top coat (left). The short dwell time, of the order of fractions of a millisecond, of the mechanically mixed powder particles in the hot core of the plasma jet is not sufficient to produce features typical of a eutectic structure. Hence the bond coat consists of seemingly unrelated streaks of intertwined titania-rich (dark) and zirconia-rich (light) areas. The spatial separation in the coating of the two components may have been augmented by the difference in powder densities that during flight in the plasma jet leads to dispersion, because gravity acts more on the denser zirconia particles than on the less-dense titania particles. Hence particles of different densities move in different trajectories. Consequently, to obtain a homogeneous bond coat, it will be necessary to melt the two phases together, and to crush and screen the resulting solid mass to yield a sprayable powder mixture. Some very small spherical particles of the zirconia-rich phase have separated from the bulk of the bond coat and now appear to float in the HAp layer. Such features can be explained by assuming a relaxation of a solidified droplet, originally subjected to an inward moving shock-wave front, caused by the impact, in the wake of a rarefaction wave moving in the opposite direction towards the shock-wave front. This relaxation leads to reliquifaction of material that now flows out sideways over the splat surface, forming a corona of tiny spherical droplets surrounding the splat [37].

Fig. 4c shows a scanning electron micrograph of a polished cross-sectional surface of a coating of series 4, with the titanium alloy substrate (right), a titania bond coat (centre) and the HAp top coat (left). The bond coat adheres exceptionally well to both the substrate and the top coat, notwithstanding the occurrence of some silicon carbide grit particles embedded into the substrate surface. The titania bond coat acts as a natural extension of the always existing thin native oxide layer covering a titanium metal surface. Because the interface metal/ceramics is supposed to facilitate unimpeded transmission of load from the implant to the surrounding bone, and because shear-induced micromotions of the HAp coating during the early healing phase can lead to a disruption of the passive oxide layer (and thus short-term increase in metal ion release to the tissue [38]), a thick titanium dioxide bond coat will likely act as a cushion against delamination caused by cyclic micromotions as well as preventing undue release of titanium ions that could induce a cytotoxic response.

Investigation of matching pairs of titanium foils and aluminium plate/epoxy/coating assemblies after separation, using scanning electron microscopy, revealed that for series 1 and 2 the titanium foil did not show any substantial adhesion of coating material, attesting to the fact that separation had occurred at the foil/coating interface. In contrast to this, scanning electron micrographs of samples of series 3 and 4 showed large amounts of bond-coat material still sticking to the titanium foil. This is indicative of the strong adhesion of titania to the substrate.

6. Conclusion

A novel peel adhesion strength test performed on 100 μm Ti6Al4V foils plasma sprayed with hydroxyapatite on top of thin (10–15 μm) biocompatible ceramic bond coats based on titania, as well as on a eutectic mixture of titania and non-stabilized zirconia, showed for such coating systems a statistically significant increase in adhesion strength. This may be explained by the development of very thin well-adhering reaction layers based on calcium titanates, such as perovskite or calcium dititanate, and calcium zirconate, that maintain the integrity of the HAp/bond coat system during peel-test loading. In this way a chemical bonding is achieved that supports mechanical bonding by interlocking of particle splats into asperities of roughened implant surfaces typical of plasma-sprayed coatings. Because such chemically very stable bond coats act as natural extensions of the extremely thin native oxide layer covering a titanium metal surface, they provide an improved chemical barrier against the *in vivo* release of titanium ions to the surrounding tissue, as well as a cushion against stresses imposed during cyclic micromotions in the early phases of the healing process after implantation. Because the bond coats also impede heat transfer into the metallic substrate during plasma spraying, thus acting as a thermal barrier, the subsequently sprayed molten hydroxyapatite splat will cool more slowly thus avoiding formation of amorphous calcium phosphate (ACP) that would result in a concurrent increase of resorption resistance against aggressive body fluid.

Acknowledgements

The support of the first author (H.K.) by the Studienstiftung des deutschen Volkes (Education Foundation of the German People) during a 4 mon student visit to the Department of Metals and Materials Engineering, University of British Columbia, Vancouver, BC, Canada is gratefully acknowledged. One of the authors (R.B.H.) is indebted to the German Federal Ministry of Education, Research, Science and Technology (BMBF) for sponsoring a 4 mon sabbatical at the Department of Chemical and Materials Engineering, University of Alberta, Edmonton, Alberta, Canada within the auspices of the German–Canadian Agreement on Scientific and Technological Cooperation, during which part of this work was carried out. Thanks are also due to Dr Walter Kunert, Freiberger Nichteisen-Metall GmbH, Freiberg, Germany, who kindly granted access to the plasma-spray equipment, and to Dr N. Dorin Ruse and Ms Edith Breslauer, Faculty of Dentistry, University of British Columbia, for providing access to the Instron universal testing machine. The microstructural investigations were performed at the Department of Chemical and Materials Engineering, University of Alberta, Edmonton, Alberta. The authors are indebted to Professor Michael L. Wayman of the above department for granting access to the electron microscope.

Appendix. Calculation of the peel force

The force, F, recorded as a function of the crack position is a linear combination of four components: (i) the force required to separate the foil from the coating (peel force G), (ii) the deadweight (D), (iii) the force of rolling friction in the bearings of the jig (f), and (iv) the plastic work required to bend the foil per increment of peeled coating (U_b/dx). Hence, the recorded force F can be represented by

$$F = G + D + f + (U_b/dx) \tag{A1}$$

Sexsmith [28, 29] suggested the use of calibration curves obtained from foils prepared in an identical manner to the sprayed foils, but without the coating. In this way, the plastic work of bending and the frictional force could be eliminated from Equation A1 assuming that the two kinds of foil had identical mechanical properties, and that the same jig was being used. The first assumption may not be justified when exposure to high temperature during plasma spraying drastically alters the mechanical properties of the foil, or when bending of some foils results in work hardening [27]. Also, the process of calibration and foil preparation is rather time consuming.

For these reasons, Breslauer and Troczynski [30] modified the originally suggested peel-adhesion test [25] by changing the deadweight, D, as the crack front progresses along the length of the coating. Hence the need for preparing a calibration foil was eliminated. The method can be described in the following way.

The frictional force, f, is proportional to the total force, F, and can be described by $f = \mu F$, where μ is the coefficient of (rolling) friction. The plastic work of bending is a function of the applied force, and proportional to the width of the sample, w. Thus, Equation A1 can be rewritten as

$$F(1 - \mu) = G + D + \alpha w \tag{A2}$$

where α is the plastic work expended per unit width per unit length of the foil. If the values of the total force, F, are plotted against the values of the deadweight, D, the coefficient of friction, μ, can be obtained from the slope of the straight line as $1/(1 - \mu)$ and the numerical value α can be obtained from the intercept with the F-coordinate for $D = 0$ as $G + \alpha w$. Furthermore, as shown in Fig. A1, the intercept of the F versus D line with the D coordinate for $F = 0$ gives the numerical value of the peel force, G, under the assumption that for $F = 0$ the plastic work $\alpha w = 0$.

In the present work, the values of F and D (N) were divided by the width of the foil (m) to eliminate the

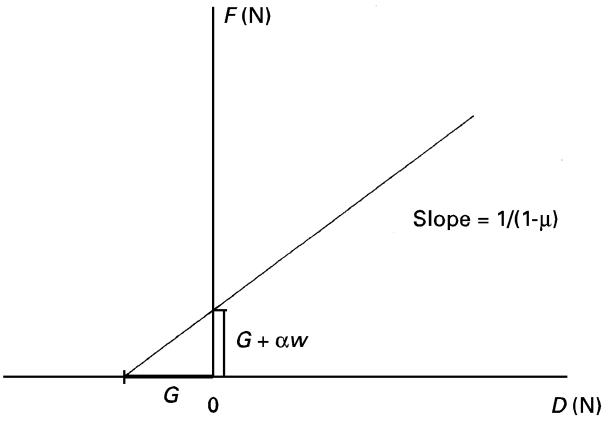

Figure A1 Schematic illustration showing the estimation of the peel force, G, from a plot of the total force, F, versus the deadweight, D.

variations in peel strength arising from variations of the width of the peeled foils. Hence the intercept of the F versus D line with the D coordinate is the normalized peel strength G/w ($\mathrm{N\,m^{-1}}$).

References

1. K. de GROOT, R. T. G. GEESINK, C. P. A. T. KLEIN and P. SEREKIAN, *J. Biomed. Mater. Res.* **21** (1987) 1375.
2. C. P. A. T. KLEIN, P. PATKA, H. B. M. van der LUBBE, J. G. C. WOLKE and K. de GROOT, *ibid.* **25** (1991) 53.
3. H. CAULIER, J. P. C. M. van der WAERDEN, J. G. C. WOLKE, W. KALK, I. NAERT and J. A. JANSEN, in "Materials in Clinical Application", edited by P. Vincenzini (Techna Srl, 1995) p. 477.
4. R. McPHERSON, N. GANE and T. J. BASTOW, *J. Mater. Sci. Mater. Med.* **6** (1995) 327.
5. R. B. HEIMANN, T. A. VU and M. L. WAYMAN, *Europ. J. Mineral.*, **9** (1997) 597.
6. K. SØBALLE, H. B. RASMUSSEN, E. S. HANSEN and C. BUENGER, *Acta Orthop. Scand.* **63**(2) (1992) 128.
7. C. Y. YANG, B. C. WANG, E. CHANG and J. D. WU, *J. Mater. Sci. Mater. Med.* **6** (1995) 249.
8. R. B. HEIMANN and T. A. VU, *J. Thermal Spray Technol.*, **6** (2) (1997) 145.
9. R. B. HEIMANN, "Plasma Spray Coating, Principles and Applications" (VCH, Weinheim, 1996).
10. J. WENG, X. LIU, X. ZHANG and X. JI, *J. Mater. Sci. Lett.* **13** (1994) 159.
11. H. JI, C. B. PONTON and P. M. MARQUIS, *J. Mater. Sci. Mater. Med.* **3** (1992) 283.
12. M. L. PEREIRA, A. M. ABREU, J. P. SOUSA and G. S. CARVALHO, *ibid.* **6** (1995) 523.
13. H. TOMAS, G. S. CARVALHO, M. H. FERNANDES, A. P. FREIRE and L. M. ABRANTES, *ibid.* **7** (1996) 291.
14. K. SØBALLE, *Acta Orthop. Scand.*, **64** (255) (1993) 58.
15. D. LAMY, A. C. PIERRE and R. B. HEIMANN, *J. Mater. Res.* **11** (1996) 680.
16. T. A. VU and R. B. HEIMANN, Second Interim Report SMWK Project no. 7541.82-0390/414, 15 February 1996.
17. P. F. KEETING, M. J. OURSLER, K. E. WIEGAND, S. K. BONDS, T. C. SPELSBERG and B. L. RIGGS, *J. Bone Miner. Res.* **7** (1992) 1281.
18. L. L. HENCH, *Thermochimica Acta* **280/281** (1996) 1.
19. M. TANAHASHI, T. YAO, T. KOKUBO, M. MINODA, T. MIYAMOTO, T. NAKAMURA and T. YAMAMURO, *J. Mater. Sci. Mater. Med.* **6** (1995) 319.
20. Y. EBISAWA, T. KOKUBO, K. OHURA and T. YAMAMURO, *ibid.* **1** (1990) 239.
21. K. OGAWA, N. NAGATA and T. YOGORO, *Onoda Research Report* **43** (1991) 2nd book, No. 125, 46 (in Japanese).
22. H. KURZWEG, PhD thesis, Freiberg University of Mining and Technology, Germany, in progress.
23. R. B. HEIMANN, "Plasma Spray Coating. Principles and Applications" (VCH, Weinheim, 1996) p. 248–61.
24. M. J. FILIAGGI, N. A. COMBS and R. M. PILLIAR, *J. Biomed. Mater. Res.* **25** (1991) 1211.
25. M. SEXSMITH and T. TROCZYNSKI, *J. Thermal Spray Technol.* **3** (1994) 404.
26. A. CROCOMBE and R. ADAMS, *J. Adhes.* **12** (1981) 127.
27. M. SEXSMITH, T. TROCZYNSKI and E. BRESLAUER, *J. Adhes. Sci. Technol.*, **11** (2) (1997) 141.
28. M. SEXSMITH, MASc thesis, The University of British Colmbia (1995).
29. M. SEXSMITH and T. TROCZYNSKI, *J. Thermal Spray Technol.* **5** (1996) 196.
30. E. BRESLAUER and T. TROCZYNSKI, *ibid.*, submitted.
31. L. E. SAMUELS, "Metallographic Polishing by Mechanical Methods" (ASM, Metals Park, OH, 1982) p. 288.
32. R. STORM, "Wahrscheinlichkeitsrechnung, mathematische Statistik und statistische Qualitätskontrolle" (Fachbuchverlag, Berlin, 1995) pp. 253–6.
33. M. O. FIGUEIREDO and A. CORREIA DOS SANTOS, in "Zirconia '88. Advances in Zirconia Science and Technology", edited by S. Meriani, C. Palmonari (Elsevier Applied Sciences, London, New York, 1989) p. 81.
34. S. F. HULBERT, S. J. MORRISON and J. J. KLAWITTER, *J. Biomed. Mater. Res.* **6** (1972) 347.
35. C. C. RIBEIRO, M. A. BARBOSA, A. A. S. C. MACHADO, A. TUDOR and M. C. DAVIES, *J. Mater. Sci. Mater. Med.* **6** (1995) 829.
36. D. MATEJKA, V. PALKA and I. INFNER, in "IV. Workshop Plasmatechnik", edited by G. Nutsch 14–15 October 1996 (TU, Ilmenau, 1996).
37. J. M. HOUBEN, PhD thesis, Technical University Eindhoven, The Netherlands (1988).
38. L. L. HENCH and J. WILSON, "An Introduction to Bioceramics" (World Scientific, London, 1993).

Received 24 March
and accepted 22 May 1997